STUDIES IN THE PROPERTIES OF HEAT INSULATING BUILDING MATERIALS

Part II.—The Thermal Conductivity of Binary Mixtures with Particular Reference to Cellular Concrete

Mazhar Mahmood Qurashi and A. K. M. Ahsanullah

Central Laboratories, Pakistan Council of Scientific and Industrial Research, Karachi

Introduction

In Part I of this paper,[1] some measurements were presented on the physical properties of concrete mixtures composed of cement and rice husk ash in various proportions, ranging from 5:1 upto 1:20 by volume. Especially interesting was the curve for thermal conductivity against the composition of the mix, which exhibited an intermediate minimum followed by a maximum, as shown in Fig. 2 in Part I of this paper. It is easily seen that these mixtures essentially form cellular concretes because the ash is extremely porous with a cellular structure (Fig. 6(a) below).

In a system of this type, the thermal conductivity of any particular composition depends on three distinct factors, namely, (1) the law governing the thermal conductivity of a simple mixture of the constituents whithout any changes in volume or chemical interaction, (2) the change in density caused by the purely mechanical volume changes resulting from mixing, setting, etc., and (3) the formation of new products by chemical interaction between the constituents of the mix.

The first factor appears to be the dominant one in the case of concretes of cement and rice husk ash, the second and third coming next in importance. Therefore it was thought advisable first to investigate, both theoretically and experimentally, the thermal conductivities of cellular concretes, and then to apply these results to elucidate the behaviour of the complex cement-rice-husk-ash system, which comprises at least three components, viz., cement, air, and the silica of the ash. In order to analyse the first factor, we must find an accurate expression for the thermal conductivity of intimate mixtures of two substances of thermal conductivities K_a and K_b mixed in various proportions x_a and x_b by volume.

1. Examination of Previous Formulae

Two formulae for the thermal conductivity of porous materials are extant in the literature. The one derived by Russell[2] for rectilinear flow through a cubic array of cubical pores of conductivity K_g embedded in a solid of conductivity K_s gives

$$\frac{K_s}{K} = 1 - P^{1/3} + P^{1/3} \left/ \left\{ (1 - P^{2/3}) + (K_g/K_s) P^{2/3} \right\} \right.$$

(1a)

where the porosity $P = (\rho_s - \rho)/(\rho_s - \rho_g)$.

Since $K_g/K_s << 1$, this makes

$$K \simeq K_g + K_s (1 - P^{2/3}).$$

In order to test the applicability of equation 1(a), comparative plots against $(1 - P^{2/3})$ have been made in Fig. 1 for the calculated values (curve I) for cellular concretes and of the standard data (solid circles) given in the literature,[3] K_g being taken as 0.60×10^{-4} cal.cm.$^{-1}$ sec.$^{-1}/°$C. The agreement can only be described as poor, especially
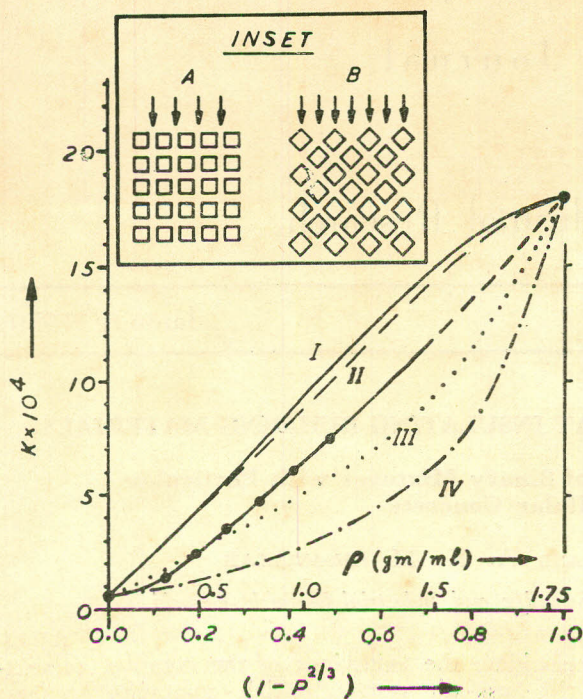
Fig. 1.—Comparative graphs of the thermal conductivity ($K \times 10^4$ cal. cm.$^{-1}$ sec.$^{-1}$/$^\circ$C.) of cellular concretes against $(1 - P^{2/3})$, where P is the porosity. The solid circles are the experimental points, and the four graphs labelled I to IV are the values calculated on the basis of:

   I.   Russell's formula for the arrangement 'A' in the inset.
  II. Maxwell and Raleigh's formula.
 III. Flow along a face-diagonal in Russell's arrangement, as shown at 'B' in the inset.
 IV. Flow along a body-diagonal in Russell's arrangement.

at high porosity, and cannot be accounted for by any allowance for the fact that the solid phase is taken as the concrete of density 1.76, which has a porosity of about 0.2. The other equation given in the literature is

$$K/K_s = \left\{ 1 - (1 - b\, K_g/K_s)P \right\} \Big/ \left\{ 1 + (b - 1)P \right\}$$

$$(1b)$$

with $b = 3\,K_s/(2\,K_s + K_g)$, and was originally derived rigorously by Maxwell[4] and later by Rayleigh[5] for the electrical conductivity of a cubic array of spherical particles in a continuous medium. The values of K obtained from this second formula are shown by the broken curve II in Fig. 1, and give an insignificant improvement on Russell's formula.

The unexpectedly large divergence of the above theoretical formulae from the experimental measurements can be traced to the use of a model with an over-symmetrical arrangement of the pores, thus providing continuous channels of the

highly conducting solid medium in directions parallel to the cube edges of the pore lattice as shown at 'A' in the inset to Fig. 1. Moreover, in this highly symmetrical arrangement, very different values are obtained for the conductivity when rectilinear heat flow is considered parallel to the face diagonal of the pore lattice, as shown at 'B' in the inset to Fig. 1. A calculation for this case under the assumptions made in Russell's derivation gives the dotted line curve III, which is in rough agreement with the experimental data. In a similar manner, an approximate calculation for flow along the body diagonal of the lattice gives the lowest (chain-dotted) curve IV, which again deviates markedly from the experimental values.

In view of the above results, it was considered necessary to set up a better model for a homogeneous mixture of two substances, such that the straight continuous channels found in the arrangement discussed above are done away with. Starting with simple composite slabs of the two substances, nearly isotropic blocks can be designed by progressive three-dimensional stacking of the slabs, thus providing a close approach to a homogeneous random mixture of the two components. The principal thermal conductivities are calculated for successive stackings, and a good approach to the ultimate law for a homogeneous mixture is obtained in the third step, this law being in excellent agreement with experimental data.

2. Derivation of the Theoretical Formula for Conductivity of a Simple Homogeneous Mixture

Consider first a composite slab made up of several alternate layers of substance A of thickness δ_a and conductivity K_a, and substance B of thickness δ_b and conductivity K_b (Fig. 2(a)). Such a slab is not isotropic, and its equivalent conductivity, $K_\perp$, for heat flowing perpendicular to the layers (Fig. 2(a)) is different from the equivalent conductivity, $K_{||}$, for heat flowing in the two other principal directions both parallel to the layers (Fig. 2(b)). Figure 2(c) shows schematically the three principal directions for the conductivities, and this presentation indicates that, if several slabs of the type shown in Fig. 2 are stacked together in a three-dimensional array using all the three orientations at random, then, for heat flowing along any one of the principal axes of the array, there will be twice as many slabs in which heat flows parallel to the layers as there are slabs in which the heat flow is perpendicular to the layers. It follows that the resultant conductivity will be a mean of $K_\perp$ and $K_{||}$, weighted in the ratio of
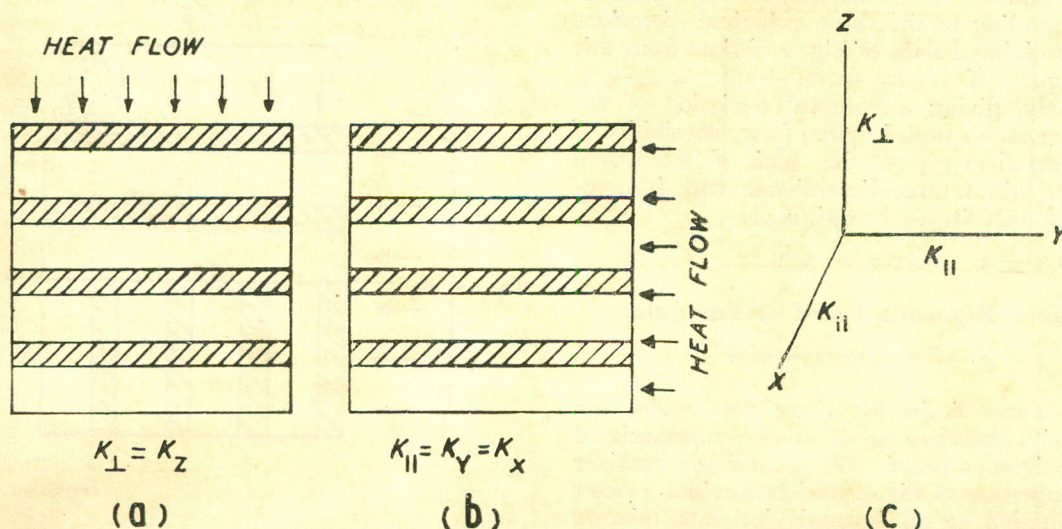
Fig. 2.—Schematic representation of the heat flow in the three principal directions through a composite slab of alternate layers of two materials, A and B: (a) heat flow$_\perp$ layers (b) heat flow$_{\parallel}$ layers (c) the three principal conductivities.

1 to 2. $K_\perp$ and $K_{\parallel}$ are readily calculated and from these values we shall be able to put down the first approximation to the conductivity of an isotropic mixture of the two substances.

$K_\perp$ and $K_{\parallel}$ can be calculated by the usual methods for heat flowing through slabs in series and in parallel (cf. flow of electric current through conductors), and the following formulae are obtained:

$$1/K_\perp = x_a/K_a + x_b/K_b = x_a/K_a + (1 - x_a)/K_b \quad (2a)$$
$$K_{\parallel} = x_a K_a + x_b K_b = x_a K_a + (1 - x_a) K_b. \quad (2b)$$

It is seen that $K_\perp$ is made up of K_a and K_b in harmonic proportion, while $K_{\parallel}$ is made up of K_a and K_b in arithmetic proportion. These formulae for $K_\perp$ and $K_{\parallel}$ can be combined into the general formula,

$$\frac{K^\varepsilon - 1}{\varepsilon} = x_a \frac{K_a{}^\varepsilon - 1}{\varepsilon} + x_b \frac{K_b{}^\varepsilon - 1}{\varepsilon}, \quad (3)$$

$K_\perp$ corresponding to $\varepsilon = -1$, and $K_{\parallel}$ to $\varepsilon = +1$. (The term $-1/\varepsilon$ on either side of formula (3) cancels out when $\varepsilon \neq 0$, while for $\varepsilon = 0$ this formula reduces to $\ln K = x_a \ln K_a + x_b \ln K_b$). If now a mean were to be taken of $K_\perp$ and $K_{\parallel}$ with equal weights, it is easily seen that the resultant formula* would closely correspond to (3) with

$\varepsilon = 0$ (mean of -1 and $+1$), i.e. to the formula $\ln K = x_a \ln K_a + x_b \ln K_b$, i.e.

$$K = K_a{}^{x_a} K_b{}^{x_b} \quad (5)$$

This is the formula for mixing by geometric proportion, and is quite to be expected, because it is well known that the geometric mean of two quantities is also the geometric mean of their arithmetic and harmonic means.

In our case, however, Fig. 2(c) requires that we take the weighted mean with weights of 1 and 2 for $K_\perp$ ($\varepsilon = -1$) and $K_{\parallel}$ ($\varepsilon = +1$), respectively. We may therefore expect that the resultant formula will be a special case of (3) with $\varepsilon = (1/3 \times (-1) + 2/3 \times 1) = 1/3$, i.e.

$$\frac{K_{mix}{}^{1/3} - 1}{1/3} = x_a \frac{K_a{}^{1/3} - 1}{1/3} + x_b \frac{K_b{}^{1/3} - 1}{1/3}, \quad (6)$$

$$\text{or} \quad K_{mix}{}^{1/3} = x_a K_a{}^{1/3} + x_b K_b{}^{1/3}. \quad (7)$$

$$\times \frac{x_a K_a + x_b K_b}{x_a K_b + x_b K_a}$$

$$= \left(K_a{}^{x_a} K_b{}^{x_b} \right)^2 \left\{ \left(x_a \left(\frac{K_a}{K_b} \right)^{x_b} \right. \right.$$

$$\left. \left. + x_b \left(\frac{K_b}{K_a} \right)^{x_a} \right) \middle/ \left(x_a \left(\frac{K_b}{K_a} \right)^{x_b} + x_b \left(\frac{K_a}{K_b} \right)^{x_a} \right) \right\} \quad (4)$$

and the factor in curly brackets is exactly equal to 1 for $x_a = 0$, $\frac{1}{2}$, and 1, and is very close to unity for intermediate values of x_a.

$$*K_\perp K_{\parallel} = K_a K_b (x_a K_a + x_b K_b)/(x_a K_b + x_b K_a)$$

$$= \left(K_a{}^{x_a} K_b{}^{x_b} \right)^2 \left(K_a{}^{x_b} K_b{}^{x_a} \middle/ K_a{}^{x_a} K_b{}^{x_b} \right)$$

It is however to be noted that the values of ε corresponding to the three principal directions for the individual slabs of Fig. 2 deviate from this mean figure of $1/3$ by $+2/3$, $+2/3$ and $-4/3$, respectively, giving a standard deviation of $2/3$ for the mean. So that, inspite of the plausibility of ε being equal to $1/3$ on the basis of the above argument with a three-dimensional array, it merely proves that, for an *isotropic mixture*,

$$\varepsilon = 1/3 \pm \alpha, \text{ where } \alpha << 2/3.$$

3. More Rigorous Proof of Formula

(i) First Approximation

The above limits for ε are very wide, and equation(7) therefore needs to be substantiated by more rigorous proof. We accordingly consider the arrangement of Fig. 3, which provides a closer approximation to an isotropic intimate mixture of the two substances, A and B. Fig. 3 comprises two composite slabs of the types shown in Figs. 2(a) and 2(b) respectively, arranged (at right angles) one above the other. Taking the y-axis and z-axis in the plane of the paper (Fig. 3) and the x-axis perpendicular to this plane, we easily find by a further application of the formulae 2 that*

$$K_x = K_{||} = x_a K_a + x_b K_b, \tag{8a}$$

$$K_y = \frac{1}{2}(K_\perp + K_{||})$$
$$= \frac{1}{2}\left\{ \frac{K_a K_b}{x_a K_b + x_b K_a} + x_a K_a + x_b K_b \right\} \tag{8b}$$

$$1/K_z = \frac{1}{2}\left(\frac{1}{K_\perp} + \frac{1}{K_{||}} \right)$$
$$= \frac{1}{2}\left\{ \frac{x_a}{K_a} + \frac{x_b}{K_b} + \frac{1}{x_a K_a + x_b K_b} \right\} \tag{8c}$$

K_y and K_z are readily shown to be very near to $K_a^{x_a} K_b^{x_b}$ in value. Thus

$$1/K_z = \frac{1}{2}\left(\frac{x_a K_b + x_b K_a}{K_a^{x_b} K_b^{x_a}} + \frac{K_a^{x_a} K_b^{x_b}}{x_a K_a + x_b K_b} \right)$$
$$\Big/ K_a^{x_a} K_b^{x_b} = (1+\delta)/\left(K_a^{x_a} K_b^{x_b} \right), \tag{8d}$$

where δ is zero for $x_a = 0,1$, and has its maximum value for $x_a = x_b = 1/2$, when it is equal to

---

*It is of course to be understood that these formulae will apply strictly only if the temperature across the dividing planes, $A_1 B_1$, $A_2 B_2$, etc. in Fig. 3 is perfectly uniform.
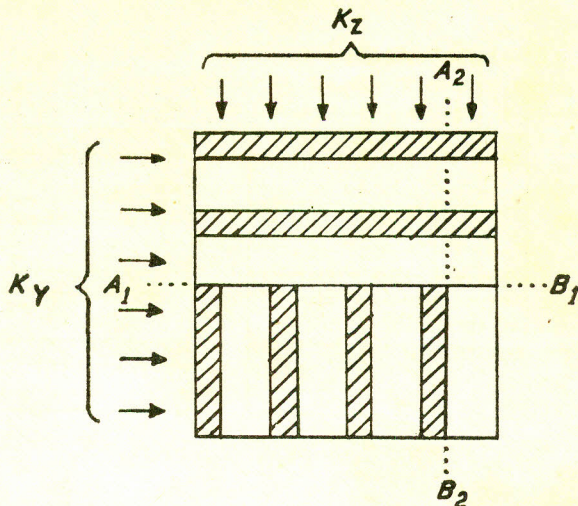

Fig. 3.—Composite block made up of two slabs of the type shown in Fig. 2 oriented so as to make the block more nearly isotropic.

$$\left\{ \frac{1}{2}\left(\frac{K_a+K_b}{2\sqrt{K_a K_b}} + \frac{2\sqrt{K_a K_b}}{K_a+K_b} \right) - 1 \right\}$$
$$= \frac{1}{2}\left(\frac{K_a+K_b}{2} - \sqrt{K_a K_b} \right)^2 \Big/ \left(\frac{K_a+K_b}{2}\sqrt{K_a K_b} \right),$$

which is only 0.13 for $K_a/K_b = 9$. Similarly

$$K_y = \frac{1}{2}\left(\frac{x_a K_a + x_b K_b}{K_a^{x_a} K_b^{x_b}} + \frac{K_a^{x_b} K_b^{x_a}}{x_a K_b + x_b K_a} \right) \times K_a^{x_a} K_b^{x_b}$$
$$= (1+\delta')K_a^{x_a} K_b^{x_b}, \tag{8e}$$

where δ' is zero for $x_a = 0,1$, and is a maximum for $x_a = x_b = 1/2$, this maximum value being the same as for δ. Thus, the mean of K_y and K_z will be equal to $(K_a^{x_a} \times K_b^{x_b})$ to a very high degree of accuracy, so that we may conclude (cf. equation(5)) that the formula for mean thermal conductivity, $K_{y,z}$, in these two principal directions corresponds to formula (3) with $\varepsilon = 0$. K_x, on the other hand, corresponds to $\varepsilon = +1$, cf. equations 8(a) and (3). If we take a random 3-dimensional stacking of the blocks of Fig. 3, the resultant K is again given by the mean of $K_{y,z}$ and K_x, weighted in the ratio of 2 to 1, and we can estimate that the value of ε in the formula for the isotropic mixture should be very close to $(2\times 0 + 1 \times (+1))/3 = 1/3$. The S.D. of this mean being now only $1/3$ for an individual block, we have proved that for the three-dimensional stacking of the blocks, $\varepsilon = 1/3 \pm \alpha$, where $\alpha << 1/3$.

(ii) Second Approximation

The above analysis is an improvement on that given in section 2, insofar as the composite block is more nearly isotropic, and therefore the values of ε for the three principal directions vary less than before. A further improvement is effected by considering a block of the type shown in the inset to Fig. 4, which consists of slabs arranged together in three different orientations so as to give almost the same thermal conductivity in each of the three principal directions. It is seen that in each of these directions, the heat flow is parallel to the constituent layers in two of the slabs, and is perpendicular to these layers in the third. Therefore we have

$$K_{x,y} = K_x = K_y = 2/3\, K_{\parallel} + 1/3\, K_{\perp}$$
$$= 2/3\,(K_a x_a + K_b x_b) + 1/3\,\frac{K_a K_b}{x_a K_b + x_b K_a}, \qquad (9a)$$

and

$$1/K_z = \frac{2/3}{x_a K_a + x_b K_b} + \frac{x_a K_b + x_b K_a}{3\,K_a K_b} \qquad (9b)$$

If we denote the value of K calculated from equation (7) by K_{ideal}, then

$$K_{x,y} - K_{ideal}$$
$$= \frac{2\,K_a K_b (x_a{}^2 + \tfrac{1}{2} + x_b{}^2) + 2 x_a x_b (K_a{}^2 + K_b{}^2)}{3(x_a K_b + x_b K_a)}$$
$$\qquad - (x_a K_a{}^{1/3} + x_b K_b{}^{1/3})^3$$

$$= \frac{3 K_a K_b + 2 x_a x_b (K_a - K_b)^2}{3(x_a K_b + x_b K_a)}$$
$$\qquad - (x_a{}^3 K_a + x_b{}^3 K_b + 3 x_a x_b K_a{}^{1/3} K_b{}^{1/3}$$
$$\qquad\qquad \times (x_a K_a{}^{1/3} + x_b K_b{}^{1/3}))$$

$$= \left\{ \frac{K_a K_b}{x_a K_b + x_b K_a} - (x_a{}^3 K_a + x_b{}^3 K_b) \right\}$$
$$\quad + x_a x_b \left\{ \frac{2}{3}\,\frac{(K_a - K_b)^2}{x_a K_b + x_b K_a} \right.$$
$$\quad \left. - 3 K_a{}^{1/3} K_b{}^{1/3}(x_a K_a{}^{1/3} + x_b K_b{}^{1/3}) \right\}$$

Simple substitution shows that this difference is zero for $x_a = 0$ and for $x_a = 1$.
For $x_a = x_b = \tfrac{1}{2}$, it is equal to

$$\left\{ \frac{2 K_a K_b}{K_b + K_a} - \frac{K_a + K_b}{8} \right\} + \frac{1}{4}\left\{ \frac{4}{3}\frac{(K_a - K_b)^2}{K_a + K_b} \right.$$
$$\qquad \left. - \frac{3}{2}\,K_a{}^{1/3} K_b{}^{1/3}(K_a{}^{1/3} + K_b{}^{1/3}) \right\}$$

$$= \frac{1}{4}\left\{ \frac{3}{2}(K_a + K_b) - \frac{3}{2}\,K_a{}^{1/3} K_b{}^{1/3}(K_a{}^{1/3} + K_b{}^{1/3}) \right\}$$
$$+ \left\{ \frac{2 K_a K_b}{K_a + K_b} - \frac{K_a + K_b}{2} + \frac{1}{3}\frac{(K_a - K_b)^2}{K_a + K_b} \right\}$$
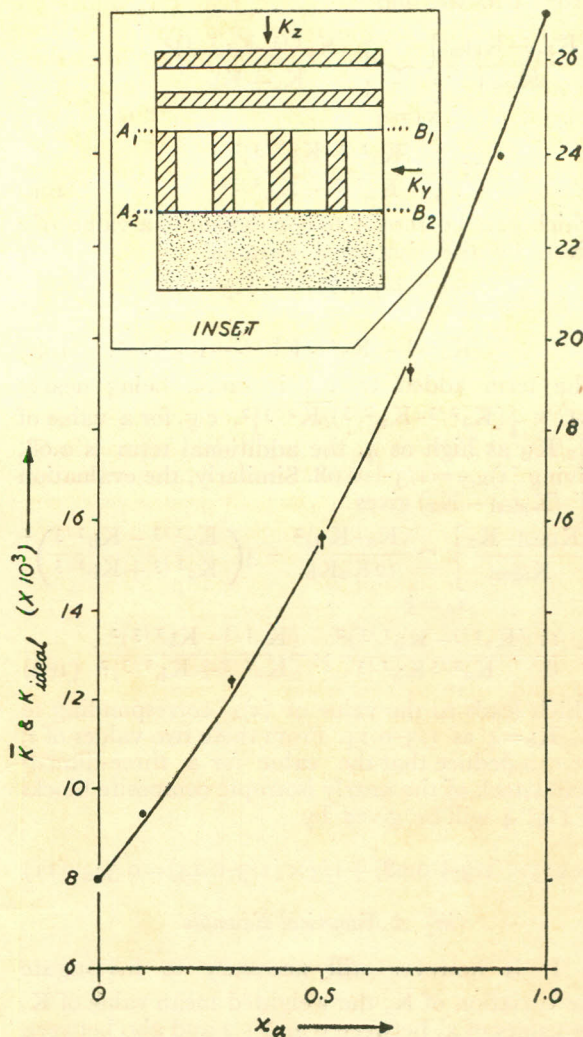

Fig. 4.—Graph showing the ideal variation of thermal conductivity for a mixture governed by the $K^{1/3}$ law proposed in this paper and the values calculated for the approximately isotropic block shown in the inset (made up of three slabs of the type sketched in Fig. 2). The dotted area indicates that the composite layers making up the slab are parallel to the plane of the paper.

$$= \frac{3}{8}\left\{ K_a - K_a{}^{2/3} K_b{}^{1/3} + K_b - K_a{}^{1/3} K_b{}^{2/3} \right\}$$
$$\quad + \left(\frac{1}{3} - \frac{1}{2} \right) \frac{(K_a - K_b)^2}{K_a + K_b}$$

$$= \frac{3}{8}(K_a{}^{1/3} - K_b{}^{1/3})(K_a{}^{2/3} - K_b{}^{2/3})$$
$$\quad - \frac{1}{6}\frac{(K_a - K_b)^2}{K_a + K_b}$$

$$= \frac{3}{4}\frac{(K_a{}^{1/3} - K_b{}^{1/3})^2}{(K_a + K_b)/2}\left\{ \frac{K_a{}^{1/3} + K_b{}^{1/3}}{2} \right.$$
$$\times \frac{K_a + K_b}{2} - \left(\frac{K_a{}^{2/3} + K_a{}^{1/3} K_b{}^{1/3} + K_b{}^{2/3}}{3} \right)^2 \right\}.$$

From this we find

$$\left\{\frac{K_{x,y}-K_{ideal}}{K_{ideal}}\right\}_{x_a=\frac{1}{2}} \simeq \frac{3}{4}\frac{(K_a^{1/3}-K_b^{1/3})^2}{K_a+K_b}$$

$$\times \frac{7}{3}\frac{(K_a^{1/3}-K_b^{1/3})^2}{K_a^{1/3}+K_b^{1/3}}, \qquad (10a)$$

which can be shown to correspond to a value of ε given by the simplified formula,

$$(\varepsilon)_{x,y} = 1/3 + 7/8(K_a^{2/3}-K_b^{2/3})^2$$

$$/(K_a^{2/3}+K_a^{1/3}K_b^{1/3}+K_b^{2/3})^2. \quad (10b)$$

The term added to $1/3$ is small, being nearly $0.1 \times \{(K_a^{2/3}-K_b^{2/3})/\overline{K^{2/3}}\}^2$, e.g. for a value of K_a/K_b as high as 4, the additional term is 0.08, giving $(\varepsilon)_{x,y}=1/3+0.08$. Similarly, the evaluation of $(K_{ideal}-K_z)$ gives

$$\left\{\frac{K_{ideal}-K_z}{K_{ideal}}\right\}_{x_a=\frac{1}{2}} \simeq \frac{(K_a-K_b)^2}{12K_aK_b} - 3\left(\frac{K_a^{1/3}-K_b^{1/3}}{K_a^{1/3}+K_b^{1/3}}\right)^2$$

$$\simeq \frac{11}{8}\frac{(K_a^{1/3}-K_b^{1/3})^2}{K_a^{1/3}K_b^{1/3}} \times \frac{(K_a^{1/3}-K_b^{1/3})^2}{(K_a^{1/3}+K_b^{1/3})^2}, \quad (10c)$$

which leads to the value of $(\varepsilon)_z$ corresponding to $K_a/K_b=4$ as $1/3-0.14$. From these two values of ε, we can deduce that the value for a three-dimensional stack of the nearly isotropic composite blocks of Fig. 4 will be given by

$$\overline{\varepsilon}=2/3\times(1/3+0.08)+1/3\times(1/3-0.14)=0.34_0. \quad (11)$$

(iii) A Numerical Example

It is however still necessary to investigate the variation of $\overline{K}$, the weighted mean value of K, for values of x_a between 0 and $1/2$ and also between $1/2$ and 1.

This is best done by means of a numerical example. Taking $K_a=27\times10^{-3}$ and $K_b=8\times10^{-3}$, so that $K_a/K_b = 3.4$, $K_a^{1/3}=0.3$ and $K_b^{1/3}=0.2$

we get the values given in Table 1 for K_{ideal}, $K_{x,y}$, and K_z for different values of x_a and x_b. It is seen that $K_{x,y}$, and K_z agree within about 2% over the whole range of compositions, thus showing that the composite block of Fig. 4 (inset) approximates very well to an isotropic mixture. The sixth column gives the values of $\overline{K}$, the weighted mean of $K_{x,y}$ and K_z. These values of $\overline{K}$ are plotted in Fig. 4 as solid circles, while the short vertical lines indicate the deviations of $K_{x,y}$ and K_z from $\overline{K}$. The variation of K_{ideal} is shown by the smooth curve, from which it is apparent that (a) $\overline{K}$ is exactly equal to K_{ideal} for $x_a=0$ and 1, and also for $x_a=0.51$, (b) $\overline{K}$ deviates from K_{ideal} by at most 2%, the deviations being distributed evenly about the curve, and (c) the best value of the index ε for overall agreement with $\overline{K}$ is the one used for K_{ideal}, i.e. $1/3$.

The small discrepancies still remaining between $\overline{K}$ and K_{ideal} can be attributed to the fact that (a) oblique flow of heat has not been considered in the above analysis, and (b) the temperature over any one of the dividing planes such as A_1B_1, A_2B_2 in Fig. 4 is not strictly constant. Because the small discrepancies between $\overline{K}$ and K_{ideal} are evenly distributed about the curve for K_{ideal}, it can be anticipated that they will vanish when the defects in the analysis are removed.

4. Experimental Verification with Cellular Concretes

An excellent experimental test for the correctness of the formula derived above is in its application to the thermal conductivities of cellular materials such as cellular concrete, cork, etc., which can be considered to be isotropic mixtures of the entrapped air with the cement, wood, or other material involved. Since the conductivity of cement is of the order of 1.5×10^{-3} calories cm.$^{-1}$ sec^{-1}/°C., while that of air is 0.06×10^{-3}, the conductivities of cellular concretes will cover

Table 1.—Comparison of K_{ideal} with $K_{x,y}$, K_z and $\overline{K}$ for $\widetilde{K}_a=27\times10^{-3}$ and $K_b=8\times10^{-3}$.

x_a	x_b	$K_{ideal}\times10^3$	$K_{x,y}\times10^3$	$K_z\times10^3$	$\overline{K}\times10^3$	$\dfrac{\overline{K}-K_{ideal}}{K_{ideal}}$	
0.0	1.0	8.00	8.00	8.00	8.00	0.0%	
0.1	0.9	9.26	9.47	9.43	9.46	+2.1%	
0.3	0.7	12.17	12.51	12.27	12.43	+2.1%	Root mean
0.5	0.5	15.63	15.78	15.36	15.64	+0.1%	square value
0.7	0.3	19.68	19.45	19.07	19.32	-1.8%	$=\pm 1.3\%$
0.9	0.1	24.40	24.00	23.90	23.97	-1.8%	
1.0	0.0	27.00	27.00	27.00	27.00	0.0%	

a decade of values from 1×10^{-3} to 0.1×10^{-3} cal. cm.$^{-1}$ sec.$^{-1}$/°C., and so a precise estimate can be made of the best value of the index ε that fits the experimental data. For a two-component system such as air and cement, the density ρ is given by $\rho = x_{air} \, \rho_{air} + x_{cement} \, \rho_{cement} = x_{cement} \, \rho_{cement}$ (where $x = $ parts by volume), to a sufficient accuracy because $\rho_{air} = 0.001$ g./ml. while $\rho_{cement} \sim 2$ g./ml. Thus we may take the density ρ of the cellular concrete as varying linearly with the porportion of cement by volume. Table 2 below gives the standard measured values of ρ and K for several cellular cements as given in the report of the Division of Building Research of the C.S.I.R.O. Australia[3] (1954), the standard deviation of the values of K being about 4%. In Fig. 5(a), K and also its logarithm are plotted against the density ρ, and it is seen that both graphs show a strong curvature, but in opposite directions. Since $\ln K = \lim_{n \to 0} (K^n - 1)/n$, the function $\ln K$ clearly corresponds to the value 'o' of the index ε. It follows that the correct value of the index ε lies between 1 (K–plot linear) and o (lnK plot linear). In order to determine the precise value of ε, it is useful to calculate the function $\varphi_\varepsilon(K) = ((K \times 10^4)^\varepsilon - 1)/\varepsilon$ for two values of ε, viz. 0.30 and 0.35, lying on either side of the expected value 1/3. (This function has the special feature that its value for $K \sim 1 \times 10^{-4}$ is practically independent of ε.) The corresponding points are plotted in Fig. 5(b), and are seen to lie fairly well on the straight lines joining the extreme points drawn therein. However, a close inspection of the deviations of the experimental points from the straight lines shows that they are preponderantly positive in the plot for $\varepsilon = 0.30$ and somewhat negative in the case of $\varepsilon = 0.35$. Therefore the best experimental value of ε may be taken as 0.33 ± 0.02, which is in excellent agreement with the theoretical value of 1/3 derived in equations (6) and (7) and proved more rigorously in section 3. This firmly establishes the $K^{1/3}$ law
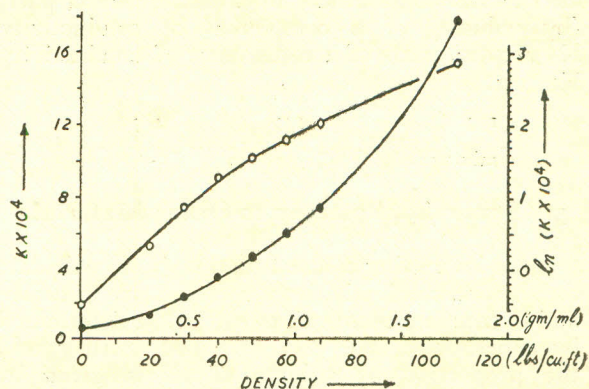
(a)
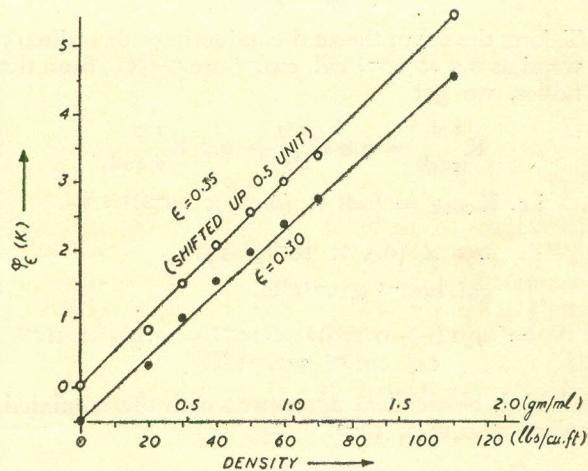
(b)

Fig. 5.—Comparison of experimental data on cellular concretes with the theoretically deduced $K^{1/3}$ law:

(a) graphs of K_{expt} and $\ln (K_{expt})$ against density for cellular concretes: K_{expt} solid circles; $\ln (K_{expt})$, hollow circles.

(b) graphs of $\varphi_\varepsilon(K) = ((K \times 10^4)^\varepsilon - 1)/\varepsilon$ for two values of ε, showing that the best value of ε lies in between them.

TABLE 2.—MEASURED CONSTANTS FOR CELLULAR CONCRETE (AT 75 °F.) SHOWING THE APPLICABILITY OF THE $K^{1/3}$ LAW.

Density, ρ (lbs./cu. ft.)	0.05 (Air)	20	30	40	50	60	70	110 (breeze concrete)
K { British units cal. cm.$^{-1}$ sec.$^{-1}$/ °C. $\times 10^4$ ..		0.4	0.7	1.04	1.38	1.77	2.17	5.2
	0.6_0	1.3_8	2.4_1	3.58	4.7_5	6.0_9	7.4_7	17.9
$\ln (K \times 10^4)$ ..	-0.51_0	$+0.32_2$	$+0.88_0$	1.27_5	1.55_9	1.80_5	2.01_0	2.88_5
$((K \times 10^4)^{0.3} - 1)/0.3$	-0.47_3	$+0.33_9$	$+1.00_7$	1.55_3	1.98_6	2.39_6	2.75_9	4.58_7
$((K \times 10^4)^{0.35} - 1)/0.35$	-0.46_8	$+0.34_0$	$+1.03_0$	1.60_8	2.07_2	2.51_8	2.91_8	4.98_5

for thermal conductivity of a mixture of x_a parts (by volume) of a component of conductivity K_a with x_b parts of a component of conductivity K_b, viz.

$$K_{mixture}^{1/3} = x_a K_a^{1/3} + x_b K_b^{1/3}. \tag{7}$$

5. Some Applications to Other Materials

It is interesting to use equation (7) to calculate the thermal conductivities of cork and rice husk ash, and to compare these values with those determined by experiment. For cork of density 0.16 g./ml., the proportion by volume of air is given by

$$x_{air} = 1 - \left(\frac{0.16}{\rho_{wood}} \right) = 1 - \frac{0.16}{0.8} = 0.8$$

Taking the mean thermal conductivity of ordinary wood as 0.5×10^{-3} cal. cm.$^{-1}$ sec.$^{-1}$/°C., from the tables, we get

$$K_{cork}^{1/3} = 0.8 K_{air}^{1/3} + 0.2 K_{wood}^{1/3},$$

i.e. $K_{cork} = \{0.8 \times (0.06 \times 10^{-3})^{1/3} +$

$0.2 \times (0.5 \times 10^{-3})^{1/3}\}^3$

cal. cm.$^{-1}$ sec.$^{-1}$/°C.

$$= (0.314 + 0.159)^3 \times 10^{-3} = 0.10_5 \times 10^{-3}$$
$$\text{cal. cm.}^{-1} \text{ sec.}^{-1}/°C.$$

which is in excellent agreement with the tabulated value of 0.11×10^{-3}.

Rice husk ash is essentially a lattice work of SiO_2 with air in the spaces, as appears in the photograph of Fig. 6(a). X-ray powder photographs of the ash (Fig. 6(b)) indicate that the SiO_2 is mostly in the form of cristobalite, which has a density of 2.4 g./ml. and a thermal conductivity of 18×10^{-3} cal.$^{-1}$ cm. sec.$^{-1}$/°C. However, there is a strong possibility of a certain amount of amorphous silica ($K = 4 \times 10^{-3}$ cal. cm.$^{-1}$ sec.$^{-1}$/°C.), being present, and assuming a ratio of 2:1 for these two constituents, we can estimate the effective K for the SiO_2 of the ash as $(12 \pm 4) \times 10^{-3}$ cal. cm.$^{-1}$ sec./°C. From the measured density, 0.2 g./ml., of the ash (Table 1 in Part I)[1] we get
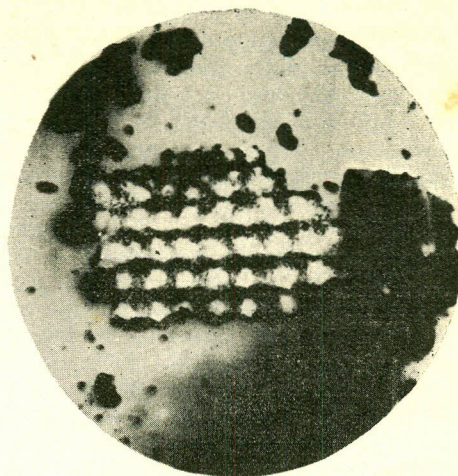

Fig. 6(a).—Photomicrograph of a particle of rice-husk ash (approximately × 100) showing its cellular structure.

$x_{SiO_2} = 0.2/2.4 = 0.08_3$, and $x_{air} = 1-0.08_3 = 0.91_7$

Therefore $K_{ash} = \{0.917 \times (0.06 \times 10^{-3})^{\frac{1}{3}}$

$+ 0.083 \times ((12 \pm 4) \times 10^{-3})^{\frac{1}{3}} \}^3$

$= (0.360 + 0.186 \pm 0.022)^3$

$= (0.16_4 \pm 0.01_9) \times 10^{-3}$ cal. cm.$^{-1}$ sec.$^{-1}$/°C.,

which compares well with our measured value[1] of 0.15 ± 0.02. It is noteworthy that a cellular concrete of the same density as the ash would have a K value of 0.11×10^{-3} as given by the graphs of Fig. 5.

The good agreement with experiment seen in these two examples affords additional support for the correctness of formula (7), which can be recast into a more useful form for this type of application, viz.

$$K_{calc} = \left\{ K_{air}^{1/3} \left(x_{air} + x_b \left(\frac{K_b}{K_{air}} \right)^{\frac{1}{3}} \right) \right\}^3$$

$$= K_{air}\{1 - x_b + x_b(K_b/K_{air})^{\frac{1}{3}}\}^3$$

$$= K_{air}\{1 + (1-P)((K_b/K_{air})^{1/3} - 1)\}^3 \tag{12}$$

with P, the porosity of the material, being given by $(\rho_b - \rho)/(\rho_b - \rho_{air}) \simeq 1 - \rho/\rho_b$, where ρ is the density of the composite material, and ρ_b that
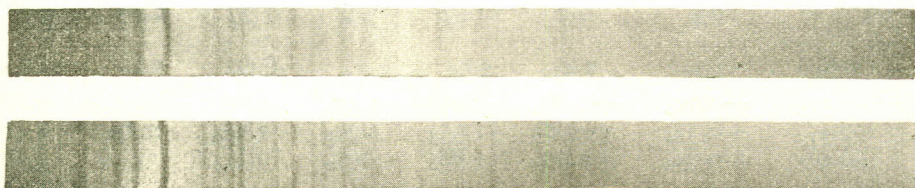

Fig. 6 (b).—X-ray powder pattern of the ash compared with a standard pattern of cristobalite (both taken with filtered CuK radiation).

of the component B. It is to be noted here that the experimental results cited above extend only upto a porosity of about 0.9. Further examination of the case of materials with higher porosities is in hand, and will be reported separately.

Acknowledgements

The authors are indebted to Mr. Sanaul Haq for taking the photomicropraph of the rice husk ash, to Mr. Sadrul Hasan Rizvi for the X-ray powder pattern of this ash, and to Mrs. D. Loman of Pansdoc for discussion of the relation with earlier work.

References

1. A.K.M. Ahsanullah, Mubarak Ahmad and Abdul Hamid Chotani, Pakistan J. Sc. Ind. Research, **1**, 53 (1958).
2. H.W. Russell, J. Am. Ceram. Soc., **18**, 1 (1935).
3. J.R. Barned, Report No. R 2 of the Division of Building Research of the C.S.I.R.O. Australia. (1946, reprinted 1954), p. 28.
4. C. Maxwell, *Treatise on Electricity and Magnetism* (Oxford University Press, London, 1873), vol. 1, p. 365.
5. W.R. Rayleigh, Phil. Mag., **5**, 481 (1892).